The International Journal of Cardiovascular Imaging (2019) 35:2147–2155
https://doi.org/10.1007/s10554-019-01679-6

ORIGINAL PAPER

Impact of lesion angle on optical coherence tomography findings and clinical outcomes after drug-eluting stent implantation in curved vessels

Shun Nakamura[1] · Shigeki Kimura[1] · Shun Nakagama[1] · Toru Misawa[1] · Masafumi Mizusawa[1] · Kazuto Hayasaka[1] · Yosuke Yamakami[1] · Keisuke Kojima[1] · Yuichiro Sagawa[1] · Keiichi Hishikari[1] · Hiroyuki Hikita[1] · Atsushi Takahashi[1] · Kenzo Hirao[2]

Received: 14 March 2019 / Accepted: 24 July 2019 / Published online: 29 July 2019

Abstract

Tortuous coronary lesions are associated with adverse outcomes after implantation of bare metal or first-generation drug-eluting stents (DESs). We investigated the impact of lesion angle on vessel wall injuries and stent apposition as assessed by optical coherence tomography (OCT) after second- and newer-generation DES implantation. We investigated 95 de novo lesions treated with a single DES (62 platinum-chromium everolimus-eluting stents and 33 bioresorbable-polymer sirolimus-eluting stents). Post-intervention OCT findings were compared between angled lesions (≥45°; n = 33) and non-angled lesions (<45°; n = 62). The 12-month clinical outcomes were also compared between the groups. Cross-sectional OCT analysis revealed that compared to non-angled lesions, angled ones had a significantly higher incidence of intra-stent dissection around the centre of the angle (19.7% vs. 10.8%, p = 0.01) and incomplete stent apposition (ISA) in the distal and proximal sub-segments (10.0% vs. 4.1%, p = 0.002; 15.3% vs. 7.9%, p < 0.001, respectively). Strut-based analysis also showed that angled lesions demonstrated a higher rate of malapposed strut in the distal and proximal sub-segments (3.0% vs. 0.9%, p < 0.001; 4.3% vs. 1.8%, p < 0.001, respectively). The 12 month clinical outcomes were comparable between the groups. Compared to non-angled lesions, angled coronary lesions were associated with a higher incidence of intra-stent dissection and ISA on post-intervention OCT after implantation of second- and newer-generation DESs.

Keywords Drug-eluting stent · Optical coherence tomography · Quantitative coronary angiography · Angled lesion

Background

The development of drug-eluting stents (DESs) has decreased the incidence of intra-stent restenosis, which used to be a key problem after bare metal stent (BMS) implantation [1], and DESs have enabled percutaneous coronary intervention (PCI) for complex coronary lesions. Nonetheless, intra-stent restenosis continues to occur in some lesions treated with DESs [2]. Additionally, stent thrombosis is a notable complication occurring after DES implantation [3]. Tortuous coronary lesions have been reported to be associated with adverse outcomes after the implantation of BMS and first-generation sirolimus-eluting stent. Park et al. showed that lesion angle larger than 45° was an independent predictor of stent fracture [4]. Hinge motion was also reported as an independent risk factor of intra-stent restenosis [5]. Second-generation DESs using biocompatible polymers and thin struts with improved conformability were expected to overcome these problems, but even these stents, namely, cobalt-chromium everolimus-eluting stent (CoCr-EES) and zotarolimus-eluting stent (ZES), showed a high rate of OCT-detected vessel wall injuries and incomplete stent apposition (ISA) in the case of angled coronary lesions [6]. In recent years, new types of DESs have been developed, including EES, which has a platinum-chromium platform

Electronic supplementary material The online version of this article (https://doi.org/10.1007/s10554-019-01679-6) contains supplementary material, which is available to authorized users.

✉ Shigeki Kimura
shigeki55@nifty.com

[1] Cardiovascular Center, Yokosuka Kyosai Hospital, 1-16 Yonegahamadori, Yokosuka, Kanagawa 238-8558, Japan

[2] Department of Cardiovascular Medicine, Tokyo Medical and Dental University, Tokyo, Japan

with high conformability, and newer-generation sirolimus-eluting stent, which is coated with a bioresorbable polymer to improve vessel wall healing after implantation [7, 8]. In the present study, we investigated the OCT findings and clinical outcomes after implantation of these latter stents in curved vessels, and we verified the clinical significance of lesion angle in newer-generation DES era.

Method

Study population

We investigated all coronary lesions treated by PCI with OCT assessment between January 2015 and December 2015 in Yokosuka Kyosai Hospital, and identified 162 lesions in 147 patients treated with a single DES—Promus coronary stent (platinum-chromium everolimus-eluting stent [PtCr-EES]; Boston Scientific, Marlborough, MN, USA) or Ultimaster coronary stent (bioresorbable-polymer sirolimus-eluting stent [BP-SES]; Terumo, Tokyo, Japan). We excluded 4 in-stent restenotic lesions, 3 left main lesions, 34 lesions with overlap stent, and 21 lesions with inadequate post-intervention OCT image quality. In patients who had more than two eligible lesions assessed by OCT during the study period, we evaluated only the first assessed lesion, thereby excluding 5 more lesions. Consequently, we analyzed 95 de novo lesions in 95 patients treated with 62 PtCr-EESs and 33 BP-SESs. This study was in accordance with the ethical standards of the institutional review committee and with the Helsinki declaration, and all the participants gave written informed consent.

Angiography and angle measurement

Quantitative coronary angiography was performed using CAAS 4.1.1 (Pie Medical Imaging, Maastricht, the Netherlands). Minimal lumen diameter (MLD), reference vessel diameter, diameter stenosis, and the length of the target lesions were measured. Post-intervention MLD was also measured, and acute gain was calculated as the difference between pre- and post-intervention MLD. In order to calculate lesion angle, a view with minimal foreshortening of the target lesion was selected, and the angle was measured in the end-diastolic and end-systolic phases (Fig. 1). We identified the cardiac cycle based on the cardiac motion in the angiography. In lesions with more than two bends, the bend with the largest angle was selected for analysis. According to the maximal angle during the cardiac cycle, the lesions were divided into an angled group (≥ 45°) and a non-angled group (< 45°). The cyclic change was calculated as the absolute difference in systolic and diastolic lesion angles, and hinge motion was defined as a cyclic change of ≥ 16°. The cut off values of lesion angle and hinge motion were determined based on the previous studies [4–6].

Interventional procedures and OCT image acquisition

For all PCI procedures, the strategy adopted was based on the operator's discretion. All patients were treated with aspirin 100 mg/day and a P2Y12 inhibitor (ticlopidine 200 mg/day, clopidogrel 75 mg/day, or prasugrel 3.75 mg/day) and received intravenous unfractionated heparin (8000–10,000 units) before the procedure. OCT images were acquired using a frequency-domain OCT system (ILUMIEN™; St. Jude Medical, Inc., St. Paul, MN, USA) as previously described [9]. An OCT imaging catheter was advanced distal to the target lesion and automatically pulled back at 18 mm/s (180 frames/s) during blood clearance by injection of contrast media or low-molecular-weight dextran. After the procedure, OCT images were analyzed using an offline review workstation (LightLab Imaging Inc., Westford, MA, USA). Cross-sectional OCT images were analyzed at 1-mm intervals through the stented site.

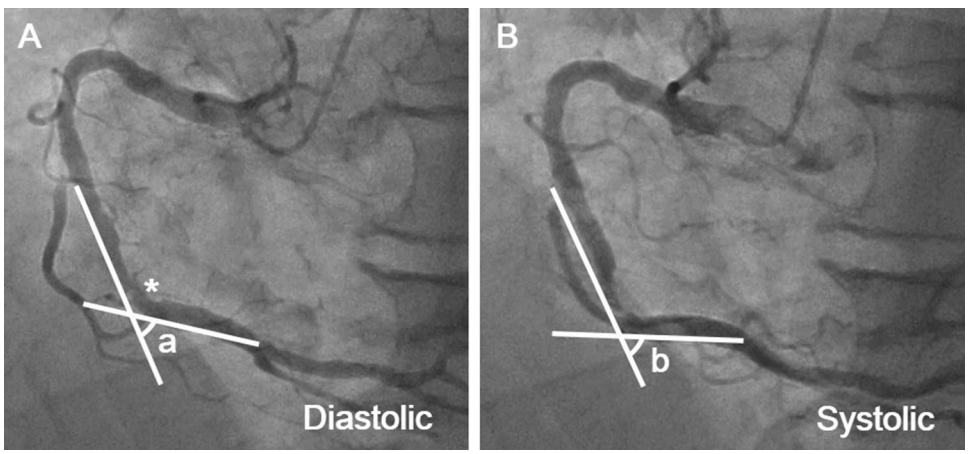

Fig. 1 Measurement of lesion angle. Measurement of lesion angle in the end-diastolic and end-systolic phases (**a** and **b**). The hinge motion was defined as [a–b] ≥ 16°. The center of lesion angle was defined as the intersection of two parallel lines (asterisk)

Image analysis and definitions

We performed stent-based and cross-sectional analysis in post-intervention OCT images. The qualitative analysis involved the presence of ISA, thrombus, intra-stent dissection, and tissue protrusion. The stent-based analysis also included stent-edge dissection. For ISA, strut-based analysis was performed to evaluate the strut-to-vessel distance of each strut in cross-sections. Slices with side branches and struts on the side branch were excluded in the cross-sectional and strut-based analysis, respectively.

Post-intervention OCT findings were defined as follows (Fig. 2a–f). ISA was considered present when the axial distance between the strut's surface and the luminal surface was larger than the combined thickness of the strut and polymer (PtCr-EES: 97 μm; BP-SES: 95 μm) [10]. Thrombus was defined as a protruding mass with an irregular surface extending beyond the stent strut into the lumen with significant attenuation behind the mass [11]. Intra-stent dissection was defined as the composite of intra-stent dissection flap and intra-stent dissection cavity, which were defined as a disruption of the luminal vessel surface in the stent segment with a dissection flap protruding in the lumen and with an underlying cavity in the vessel wall, respectively [12]. Tissue protrusion was defined as the projection of smooth-surfaced tissue into the lumen between the stent struts [11]. The volume index of thrombus and tissue protrusion was defined as the sum of area in each cross-section divided by the number of analyzed frames to adjust for the difference of stent length. Stent-edge dissection was defined as disruption of the vessel luminal surface with the presence of a visible flap within 5 mm proximal and distal to the stent [12]. Lastly, the stent eccentricity index (SEI) was determined as the minimal stent diameter divided by the maximal stent diameter [13].

The spatial distribution of these findings was recorded according to defined sub-segments (Fig. 2g) [6]: central sub-segment, that is, the 5 mm segment around the centre of the lesion angle, and peripheral segments, that is, proximal and distal sub-segments.

We also performed stent-based analysis in pre-intervention OCT findings, if available. The stent coverage area was determined by using branches as landmarks. The lipid index was defined as the sum of lipid arcs > 90° in each cross-section [14]. Thin-cap fibroatheroma was defined as a lipid-rich plaque presenting a lipid arc of > 90° and with a fibrous cap less than 70 μm thick [15]. The calcification index was also determined as the sum of calcification arcs > 90° in each cross-section.

Clinical outcomes

We evaluated the following 12 month clinical outcomes: all-cause death, cardiovascular death, non-fatal myocardial infarction, target lesion revascularisation (TLR), and definite stent thrombosis [16]. TLR was defined as ischemia-driven repeat revascularization of the stented segment [16]. Major adverse cardiovascular event (MACE) was defined as the composite of cardiovascular death and non-fatal myocardial

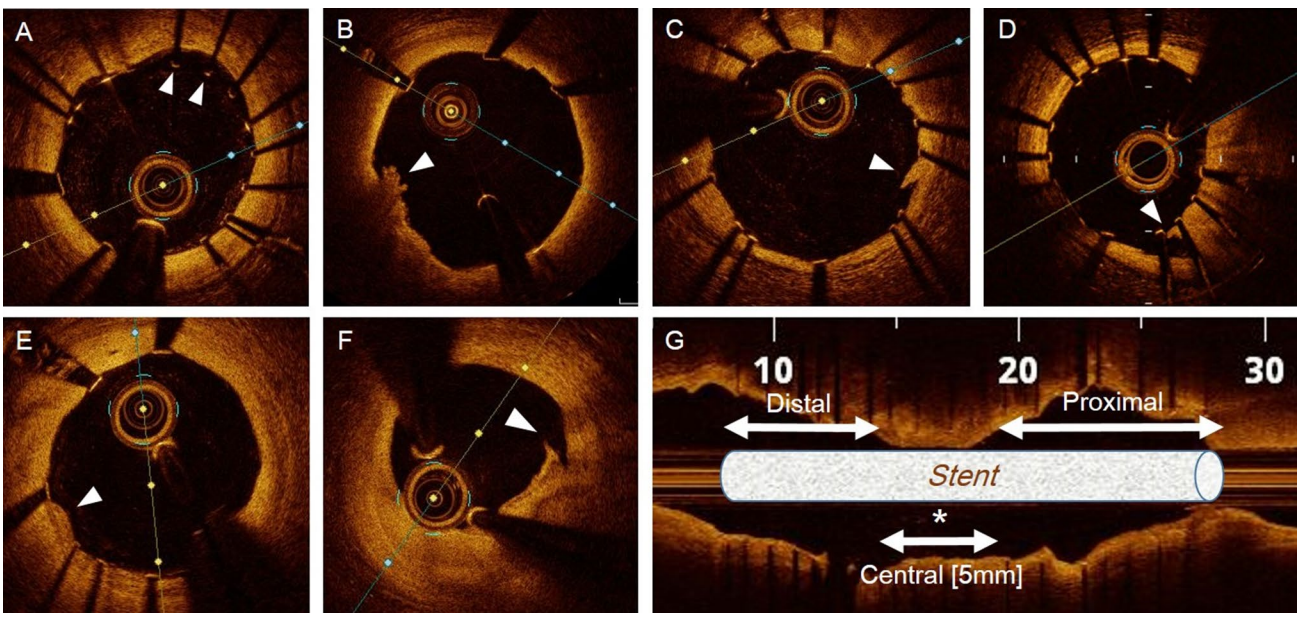

Fig. 2 Representative OCT findings and definition of stent sub-segment. Incomplete stent apposition (**a**), thrombus (**b**), intra-stent dissection flap (**c**), intra-stent dissection cavity (**d**), tissue protrusion (**e**), and stent-edge dissection (**f**). The central sub-segment was defined as a 5 mm segment around the center of lesion angle (asterisk). Other segments were defined as the proximal and distal sub-segments (**g**)

infarction. In the patients who underwent follow-up angiography within 12 months after stent implantation, quantitative coronary angiography was performed to measure MLD, reference vessel diameter, and diameter stenosis. Late loss was also calculated as the difference between post-intervention MLD and follow-up MLD.

Statistical analysis

Categorical variables were expressed as absolute frequency and percentage and were compared using the chi-square test or Fisher's exact test. Continuous variables were expressed as mean ± standard deviation for normally distributed data and as median [interquartile range] for non-normally distributed data, and they were compared using Student's *t*-test and the Mann–Whitney U-test, respectively. A two-sided P-value of < 0.05 was considered statistically significant. All statistical analyses were performed using BellCurve for Excel (Social Survey Research Information Co., Ltd. Tokyo, Japan).

Results

Baseline characteristics and interventional procedures

Among the 95 lesions in 95 patients, 33 were categorised as angled and 62 as non-angled. All clinical characteristics were comparable between the groups, except that patients with angled lesions had a lower average concentration of high-density lipoprotein cholesterol than those with non-angled lesions did (Supplementary Table 1). The median pre- and post-intervention lesion angles and cyclic changes were greater in the angled group (Table 1). The proportion of right coronary artery involvement, type B2/C lesion, and hinge motion was also significantly higher in the angled group. Further, the implanted stent length was greater in the angled group. Other lesion and procedural characteristics did not differ significantly between the groups.

Pre-intervention OCT findings

OCT images before lesion dilatation and stent implantation could be acquired in 22 and 53 lesions in the angled and non-angled groups (66.7% and 83.9%), respectively. All pre-intervention OCT findings were comparable between the groups (Table 2).

Post-intervention OCT findings

In the stent-based analysis, the post-intervention OCT findings were comparable between the groups, although the incidence of ISA, thrombus, and intra-stent dissection tended to be higher in the angled group (Fig. 3). Detailed cross-sectional analysis revealed that compared to the non-angled group, the angled group had a higher incidence of ISA in the distal and proximal sub-segments and of intra-stent dissection in the central sub-segment (Table 3). The incidence of thrombus and tissue protrusion were not significantly different between the groups. SEI was significantly smaller in all sub-segments in the angled group. Similarly, the strut-based analysis showed that strut malapposition in the distal and proximal sub-segments was more frequent in the angled group than in the non-angled group (Fig. 4a). Of all malapposed struts, the strut-to-vessel distance was < 350 μm in 91.0% (264/290 struts) and 89.6% (155/173 struts) in the angled and non-angled groups, respectively (Fig. 4b). In the angled group, post-intervention OCT cross-sectional analysis revealed that the incidence of ISA was significantly higher in the lesions with hinge motion than those without it (Supplementary Table 2).

Clinical outcomes

The 12-month clinical outcomes including MACE, TLR, and stent thrombosis were comparable between the groups (Table 4). Follow-up angiography within 12 months after stent implantation was performed in 29 and 50 patients (87.9% and 80.6%) from the angled and non-angled groups, respectively. There was no significant difference in MLD and late loss between the groups (Supplementary Table 3). No stent fracture was detected in these follow-up angiograms.

Stent type and OCT findings

Cross-sectional OCT findings for lesions treated with PtCr-EES showed that the incidence of ISA in the distal and proximal sub-segments and that of intra-stent dissection in the central sub-segment were higher in the angled group than in the non-angled group (Table 5). In contrast, no statistically significant difference was found in these parameters among lesions treated with BP-SES.

Discussion

The main findings of our study are as follows: (1) the incidence of intra-stent dissection was significantly higher around the centre of the lesion angle in angled lesions than in non-angled lesions; (2) the incidence of ISA in the distal and proximal sub-segments was higher in angled lesions than in non-angled lesions; and lastly (3) these differences did not affect the 12-month clinical outcomes.

Table 1 Lesion and procedural characteristics

	Angle (n = 33)	Non-angle (n = 62)	p-value
Angiographic characteristics			
Target lesion, n (%)			0.008
Left anterior descending artery	11 (33.3)	32 (51.6)	
Left circumflex artery	7 (21.2)	20 (32.3)	
Right coronary artery	15 (45.5)	10 (16.1)	
ACC/AHA classification, n (%)			0.005
A/B1	12 (36.4)	41 (66.1)	
B2/C	21 (63.6)	21 (33.9)	
TIMI flow grade ≤ 2, n (%)	6 (18.2)	18 (29.0)	0.25
Chronic total occlusion lesion, n (%)	0 (0)	1 (1.6)	0.65
Calcified lesion, n (%)	9 (27.3)	10 (16.1)	0.20
MLD (mm), mean ± SD	0.90 ± 0.4	0.85 ± 0.48	0.59
Reference vessel diameter (mm), mean ± SD	2.66 ± 0.56	2.51 ± 0.56	0.23
%Diameter stenosis, mean ± SD	65.9 ± 13.7	65.5 ± 19.1	0.92
Lesion length (mm), mean ± SD	14.0 ± 7.2	12.8 ± 6.5	0.42
Lesion angle, median [IQR]	63 [53–75]	26 [15–38]	< 0.001
Cyclic change, median [IQR]	13 [10–21]	4 [2–9]	< 0.001
Hinge motion, n (%)	15 (45.5)	4 (6.5)	< 0.001
Procedural characteristics			
Pre-dilatation, n (%)	31 (93.9)	58 (93.5)	0.66
Non-compliant balloon use, n (%)	3 (9.7)	6 (10.3)	0.62
Balloon diameter (mm), mean ± SD	2.6 ± 0.3	2.6 ± 0.2	0.85
Maximal pressure (atm), mean ± SD	11.1 ± 3.0	9.9 ± 3.1	0.08
Post-dilatation, n (%)	32 (100)	62 (100)	–
Non-compliant balloon use, n (%)	32 (100)	62 (100)	–
Balloon diameter (mm), mean ± SD	3.5 ± 0.5	3.3 ± 0.4	0.09
Maximal pressure (atm), mean ± SD	18.5 ± 2.8	18.1 ± 2.1	0.43
Thrombectomy, n (%)	10(30.3)	15 (24.2)	0.34
Rotational atherectomy use, n (%)	0 (0)	0 (0)	–
Stent type, n (%)			0.83
PtCr-EES	22 (66.7)	40 (64.5)	
BP-SES	11 (33.3)	22 (35.5)	
Stent diameter (mm), mean ± SD	3.2 ± 0.5	3.2 ± 0.5	0.72
Stent length (mm), mean ± SD	27.3 ± 7.2	21.8 ± 7.3	< 0.001
Post-intervention MLD (mm), mean ± SD	2.58 ± 0.59	2.54 ± 0.43	0.67
Acute gain (mm), mean ± SD	1.68 ± 0.58	1.69 ± 0.58	0.95
Post-intervention lesion angle, median [IQR]	38 [32–55]	21 [12–24]	< 0.001
Final TIMI flow grade ≤ 2, n (%)	0 (0)	3 (4.8)	0.27

ACC/AHA American College of Cardiology/American Heart Association, *TIMI* thrombolysis in myocardial infarction, *MLD* minimal lumen diameter, *PtCr-EES* platinum-chromium everolimus-eluting stent, *BP-SES* bioresorbable-polymer sirolimus-eluting stent

Mechanical stress in angled lesions

Wu et al. investigated stent conformability and the mechanical stress caused by a deployed stent in a curved vessel by using a finite element model [17]. They reported that the stent in the curved vessel model was non-conformable to the vessel, especially at its extremes, and this created gaps between the stent struts and vessel wall. They also found that the plaque stress in the curved vessel model was greater than that in the straight vessel model. The higher incidence of ISA at stent edges and intra-stent dissection in the central sub-segment in the angled group in the present study supports the findings of this ex vivo study.

The pre-intervention OCT findings of the present study showed no significant difference in the lipid index between the groups. However, the post-intervention OCT findings demonstrated a higher incidence of intra-stent dissection in the angled group than in the non-angled group, though not of

Table 2 Pre-intervention OCT findings

	Angle (n = 22)	Non-angle (n = 53)	p-value
Lipid index, median [IQR]	2423 [1710–3685]	1845 [796–3709]	0.09
Fibrous cap thickness (μm), median [IQR]	110 [85–150]	110 [90–160]	0.17
Thin-cap fibroatheroma, n (%)	8 (36.4)	14(26.4)	0.39
Thrombus, n (%)	10 (45.5)	18 (34.0)	0.35
Calcification index, median [IQR]	99 [0–945]	121 [0–554]	0.83
Minimal lumen area (mm^2), mean ± SD	1.42 ± 0.69	1.35 ± 0.61	0.64
Distal reference area (mm^2), mean ± SD	6.59 ± 3.42	5.85 ± 2.50	0.30
Proximal reference area (mm^2), mean ± SD	8.62 ± 3.55	7.18 ± 2.51	0.051

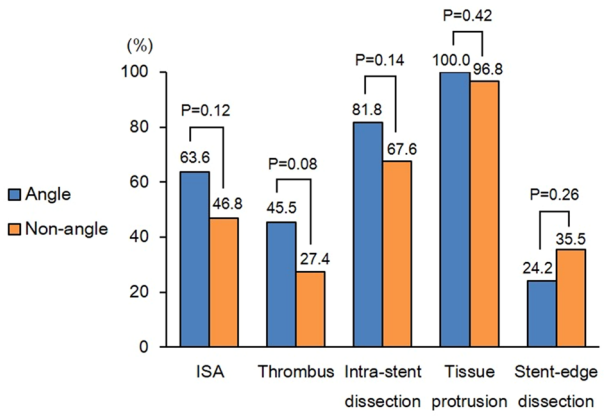

Fig. 3 Incidence of ISA and vessel injuries in stent-based analysis. *ISA* incomplete stent apposition

tissue protrusion or thrombus formation. These results imply that stents deployed in curved vessels are likely to injure fibrous plaques and cause intra-stent dissections after PCI.

Further, in our study, hinge motion was associated with lesion angulation as reported previously [6], and 19 lesions (20%) had hinge motion. In the sub-analysis among angled lesions, hinge motion was associated with the higher incidence of ISA, which implied that hinge motion might also affect the post-intervention OCT findings in addition to the lesion angulation. A previous study investigating PtCr-EES reported that the incidence of stent fracture was 1.7% and that hinge motion was an independent risk factor of this event [18]. Although the incidence of stent fracture for BP-SES has not been investigated, the absence of stent fracture in either BP-SES or PtCr-EES in the present study may suggest that the overall incidence of this event for either stent type is low.

Angled lesions and clinical outcomes

Despite the higher incidence of ISA and intra-stent dissection detected on post-intervention OCT in the angled group, the 12-month clinical outcomes were comparable between the groups, a finding that is inconsistent with those of a previous report regarding BMS [19].

The remaining of malapposed struts was reportedly associated with stent thrombosis [20], and some studies have investigated the impact of acute ISA on mid-term OCT findings. For example, Gutiérrez-Chico et al. reported that 94.9% of malapposed struts with a strut-to-vessel distance of < 350 μm were well apposed at the 6 month

Table 3 Post-intervention OCT findings in cross-sectional analysis

	Distal segment			Central segment			Proximal segment		
	Angle n = 269	Non-angle n = 395	p-value	Angle n = 152	Non-angle n = 286	p-value	Angle n = 452	Non-angle n = 606	p-value
Intra-stent dissection, n (%)	19 (7.1)	41 (10.4)	0.14	30 (19.7)	31 (10.8)	0.01	64 (14.2)	71 (11.7)	0.24
Thrombus, n (%)	10 (3.7)	10 (2.5)	0.38	2 (1.3)	10 (3.5)	0.15	35 (7.7)	41 (6.8)	0.54
Volume index ($mm^2 \times 10^2$)	0.6 ± 1.5	0.2 ± 0.6	0.065	0.3 ± 1.2	0.6 ± 2.0	0.48	2.7 ± 6.7	0.9 ± 2.4	0.054
ISA, n (%)	27 (10.0)	16 (4.1)	0.002	9 (5.9)	22 (7.7)	0.49	69 (15.3)	48 (7.9)	< 0.001
Volume index ($mm^2 \times 10^2$)	9.7 ± 31.6	4.8 ± 18.7	0.34	5.3 ± 21.3	2.5 ± 11.9	0.40	8.0 ± 14.3	3.5 ± 8.1	0.056
Tissue protrusion, n (%)	90 (33.5)	149 (37.7)	0.26	82 (53.9)	140 (49.0)	0.32	179 (39.6)	255 (42.1)	0.42
Volume index ($mm^2 \times 10^2$)	6.0 ± 9.1	7.0 ± 1.4	0.64	18.3 ± 24.6	14.4 ± 20.7	0.42	14.4 ± 19.6	10.4 ± 13.0	0.24
SEI, mean ± SD	0.86 ± 0.09	0.90 ± 0.06	< 0.001	0.86 ± 0.07	0.88 ± 0.06	0.001	0.86 ± 0.08	0.87 ± 0.06	0.001

ISA incomplete stent apposition, *SEI* stent eccentricity index

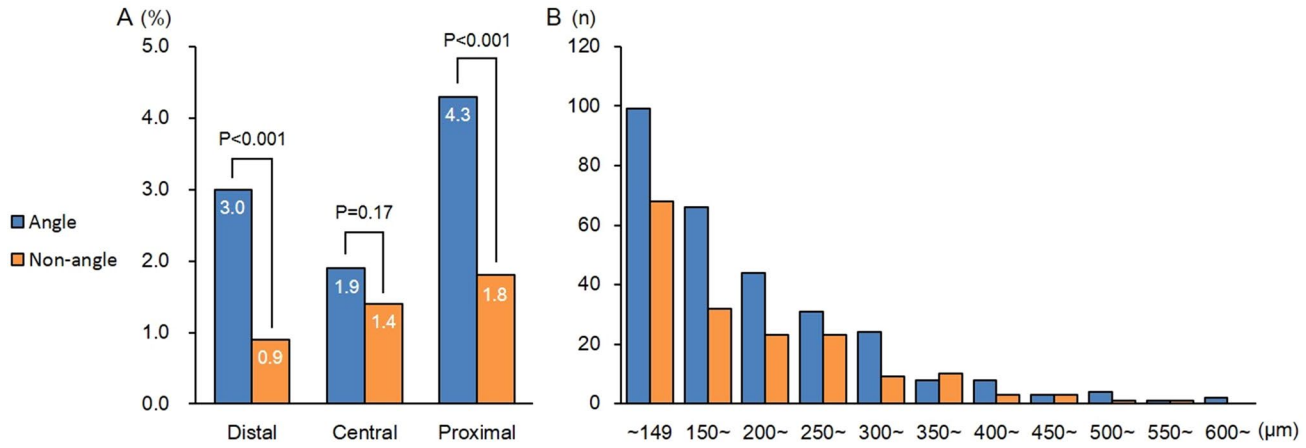

Fig. 4 Strut-based OCT analysis. Incidence of strut malapposition (**a**) and distribution of strut-to-vessel distance (**b**)

Table 4 Clinical outcomes

	Angle (n = 33)	Non-angle (n = 62)	p-value
Twelve-month outcomes, n (%)			
All-cause death	0 (0)	4 (6.5)	0.18
MACE	0 (0)	2 (3.2)	0.42
Cardiovascular death	0 (0)	2 (3.2)	0.42
Non-fatal myocardial infarction	0 (0)	0 (0)	–
Target lesion revascularization	0 (0)	1 (1.6)	0.65
Stent thrombosis	0 (0)	1 (1.6)	0.65

MACE major adverse cardiovascular event

Table 5 Stent type and OCT findings in cross-sectional analysis

PtCr-EES	Distal segment			Central segment			Proximal segment		
	Angle	Non-angle	p-value	Angle	Non-angle	p-value	Angle	Non-angle	p-value
	n = 197	n = 273		n = 106	n = 181		n = 295	n = 402	
Intra-stent dissection, n (%)	12 (6.1)	26 (9.5)	0.18	24 (22.6)	16 (8.8)	0.001	37 (12.5)	44 (10.9)	0.52
Thrombus, n (%)	8 (4.1)	7 (2.6)	0.36	2 (1.9)	9 (5.0)	0.16	23 (7.8)	27 (6.7)	0.59
ISA, n (%)	26 (13.2)	8 (2.9)	< 0.001	5 (4.7)	18 (9.9)	0.12	45 (15.3)	30 (7.5)	0.001
Tissue protrusion, n (%)	65 (33.0)	107 (39.2)	0.17	58 (54.7)	92 (50.8)	0.52	122 (41.4)	169 (42.0)	0.86
BP-SES	n = 72	n = 122	p-value	n = 46	n = 105	p-value	n = 157	n = 204	p-value
Intra-stent dissection, n (%)	7 (9.7)	15 (12.3)	0.59	6 (13.0)	15 (14.3)	0.84	27 (17.2)	27 (13.2)	0.30
Thrombus, n (%)	2 (2.8)	3 (2.5)	0.89	0 (0.0)	1 (1.0)	0.70	12 (7.6)	14 (6.9)	0.78
ISA, n (%)	1 (1.4)	8 (6.6)	0.10	4 (8.7)	4 (3.8)	0.20	24 (15.3)	18 (8.8)	0.06
Tissue protrusion, n (%)	25 (34.7)	42 (34.4)	0.97	24 (52.2)	48 (45.7)	0.46	57 (36.3)	86 (42.2)	0.26

ISA incomplete stent apposition, *PtCr-EES* platinum-chromium everolimus-eluting stent, *BP-SES* bioresorbable-polymer sirolimus-eluting stent

follow-up [21]. Inoue et al. also reported a strut-to-vessel distance of ≤ 380 μm as the cut-off value for apposition of EES [22]. In the present study, the strut-to-vessel distance was < 350 μm in 91.0% and 89.6% of all malapposed struts in the angled and non-angled groups. The findings of these previous studies seem to indicate that the extent of stent malapposition in our study may be small enough to be ignored in clinical settings.

As for intra-stent dissection, incomplete healing is reportedly associated with impaired strut coverage and apposition [12], but its clinical significance is still unclear. De Cock et al. reported that 92% of OCT-detected intra-stent

dissection flaps had healed by the 9 month follow-up [12]. Besides, newer-generation BP-SES has thin struts with an abluminal coating of biodegradable polymer, which is expected to be advantageous for early strut coverage and preventing stent thrombosis [8]. These may explain the comparable prognosis between the angled and the non-angled lesion groups.

Newer-generation DES in angled lesions

The different mechanical stresses exerted on curved vessel walls by various stent platforms have been demonstrated in ex vivo studies [23, 24] but not in vivo studies. Minami et al. showed a higher incidence of intra-stent dissection, thrombus formation, and ISA in angled lesions treated with CoCr-EES and ZES, but the study demonstrated no differences in OCT findings between the stent types [6]. In contrast, our study showed a significant association between lesion angle and the incidence of unfavourable OCT findings, that is, intra-stent dissection and ISA, in lesions treated with PtCr-EES but not those treated with BP-SES. Both these stents have thin struts (thickness, 81 and 80 μm, respectively) and a 2-link strut design. A previous bench test demonstrated that the PtCr platform had better conformability than the CoCr platform did [7], but our study showed that BP-SES with the latter platform appeared to yield favourable results in angled lesions. The stent configuration of BP-SES is designed to prevent the overlap of adjacent struts at the inner curvature of curved lesions, and this may underlie the favourable post-intervention OCT findings. Further, the newer type of polymers may also improve the vessel wall healing after stent implantation, leading to the better long-term prognosis.

Although more investigations are needed to establish the impact of stent types on the post-intervention OCT findings in angled lesions, the comparable clinical outcomes of angled lesions and non-angled lesions in the present study might suggest that lesion angulation is no longer an evident risk factor of adverse clinical outcomes with newer-generation DESs.

Limitations

The present study has some limitations. First, our study was a single-centre, retrospective study with a small sample size, and selection bias may have existed. For example, we selected relatively simple lesions which could be assessed by OCT and treated with a single stent. The small sample size has a limitation especially in the comparison of the incidence of clinical events between the groups. A larger sample is required to determine the impact of lesion angulation on clinical outcomes. Besides, in the comparison between PtCr-EES and BP-SES, the smaller number of subjects in BP-SES should be taken into account to interpret the result. Second, the lesion angle was measured in a single angiographic view. Three-dimensional reconstruction images may enable more accurate assessment of lesion angulation. Third, since pre-intervention OCT images could not be acquired in some cases, the impact of lesion morphologies on post-intervention OCT findings could not be fully evaluated. Fourth, we could not evaluate the impact of post-dilatation on the OCT findings, because post-dilatation was performed for all lesions in this study. Although the location of balloon dilatation could not be assessed, physicians performed post dilatation to acquire larger stent area and better strut apposition in the OCT-guided procedure in all cases. Finally, we only analyzed acute-phase OCT images after stent implantation and could not assess the OCT findings during follow-up. Serial OCT imaging should clarify the differences in vessel healing after stent implantation in angled and non-angled lesions.

Conclusion

For newer-generation DESs, the incidence of intra-stent dissection and ISA detection on OCT was higher for angled lesions than for non-angled lesions. However, these differences did not affect the 12 month clinical outcomes.

Compliance with ethical standards

Conflict of interest The authors declare that they have no conflict of interest.

References

1. Morice MC, Serruys PW, Sousa JE et al (2002) A randomized comparison of a sirolimus-eluting stent with a standard stent for coronary revascularization. N Engl J Med 346(23):1773–1780
2. Dangas GD, Claessen BE, Caixeta A et al (2010) In-stent restenosis in the drug-eluting stent era. J Am Coll Cardiol 56(23):1897–1907
3. Stone GW, Moses JW, Ellis SG et al (2007) Safety and efficacy of sirolimus- and paclitaxel-eluting coronary stents. N Engl J Med 356(10):998–1008
4. Park SM, Kim JY, Hong BK et al (2011) Predictors of stent fracture in patients treated with closed-cell design stents: sirolimus-eluting stent and its bare-metal counterpart, the BX velocity stent. Coron Artery Dis 22(1):40–44
5. Ino Y, Kubo T, Kitabata H, Shimamura K et al (2011) Impact of hinge motion on in-stent restenosis after sirolimus-eluting stent implantation. Circ J 75(8):1878–1884
6. Minami Y, Ong DS, Uemura S et al (2015) Impacts of lesion angle on incidence and distribution of acute vessel wall injuries and strut malapposition after drug-eluting stent implantation assessed by optical coherence tomography. Eur Heart J Cardiovasc Imaging 16(12):1390–1398
7. Menown IB, Noad R, Garcia EJ, Meredith I (2010) The platinum chromium element stent platform: from alloy, to design, to clinical practice. Adv Ther 27(3):129–141

8. Chevalier B, Smits PC, Carrie D et al (2017) Serial assessment of strut coverage of biodegradable polymer drug-eluting stent at 1, 2, and 3 months after stent implantation by optical frequency domain imaging: the discovery 1TO3 study (evaluation with OFDI of strut coverage of terumo new drug eluting stent with biodegradable polymer at 1, 2, and 3 months). Circ Cardiovasc Interv 10(12):e004801. https://doi.org/10.1161/circinterventions.116.004801
9. Sugiyama T, Kimura S, Ohtani H et al (2017) Impact of chronic kidney disease stages on atherosclerotic plaque components on optical coherence tomography in patients with coronary artery disease. Cardiovasc Interv Ther 32(3):216–224
10. Tanigawa J, Barlis P, Di Mario C (2007) Intravascular optical coherence tomography: optimisation of image acquisition and quantitative assessment of stent strut apposition. EuroIntervention 3(1):128–136
11. Otake H, Shite J, Ako J et al (2009) Local determinants of thrombus formation following sirolimus-eluting stent implantation assessed by optical coherence tomography. JACC Cardiovasc Interv 2(5):459–466
12. De Cock D, Bennett J, Ughi GJ et al (2014) Healing course of acute vessel wall injury after drug-eluting stent implantation assessed by optical coherence tomography. Eur Heart J Cardiovasc Imaging 15(7):800–809
13. Mattesini A, Secco GG, Dall'Ara G, et al (2014) ABSORB biodegradable stents versus second-generation metal stents: a comparison study of 100 complex lesions treated under OCT guidance. JACC Cardiovasc Interv 7(7):741–750
14. Zhang S, Dai J, Jia H et al (2018) Non-culprit plaque characteristics in acute coronary syndrome patients with raised hemoglobinA1c: an intravascular optical coherence tomography study. Cardiovasc Diabetol 17(1):90
15. Tanaka A, Imanishi T, Kitabata H et al (2009) Lipid-rich plaque and myocardial perfusion after successful stenting in patients with non-ST-segment elevation acute coronary syndrome: an optical coherence tomography study. Eur Heart J 30(11):1348–1355
16. Cutlip DE, Windecker S, Mehran R et al (2007) Clinical end points in coronary stent trials: a case for standardized definitions. Circulation 115(17):2344–2351
17. Wu W, Wang WQ, Yang DZ, Qi M (2007) Stent expansion in curved vessel and their interactions: a finite element analysis. J Biomech 40(11):2580–2585
18. Kuramitsu S, Hiromasa T, Enomoto S et al (2015) Incidence and clinical impact of stent fracture after PROMUS element platinum chromium everolimus-eluting stent implantation. JACC Cardiovasc Interv 8(9):1180–1188
19. Gyongyosi M, Yang P, Khorsand A, Glogar D (2000) Longitudinal straightening effect of stents is an additional predictor for major adverse cardiac events. Austrian Wiktor Stent study group and European Paragon Stent investigators. J Am Coll Cardiol 35(6):1580–1589
20. Taniwaki M, Radu MD, Zaugg S et al (2016) Mechanisms of very late drug-eluting stent thrombosis assessed by optical coherence tomography. Circulation 133(7):650–660
21. Gutierrez-Chico JL, Wykrzykowska J, Nuesch E et al (2012) Vascular tissue reaction to acute malapposition in human coronary arteries: sequential assessment with optical coherence tomography. Circ Cardiovasc Interv 5(1):20–29
22. Inoue T, Shinke T, Otake H et al (2014) Impact of strut-vessel distance and underlying plaque type on the resolution of acute strut malapposition: serial optimal coherence tomography analysis after everolimus-eluting stent implantation. Int J Cardiovasc Imaging 30(5):857–865
23. Mortier P, De Beule M, Segers P, Verdonck P, Verhegghe B (2011) Virtual bench testing of new generation coronary stents. EuroIntervention 7(3):369–376
24. Mortier P, Holzapfel GA, De Beule M et al (2010) A novel simulation strategy for stent insertion and deployment in curved coronary bifurcations: comparison of three drug-eluting stents. Ann Biomed Eng 38(1):88–99